The Correction for Thermal-Lag Effects in Sea-Bird CTD Data

JAMES MORISON AND ROGER ANDERSEN

Applied Physics Laboratory, University of Washington, Seattle, Washington

NORDEEN LARSON

Sea-Bird Electronics, Bellevue, Washington

ERIC D'ASARO AND TIM BOYD*

Applied Physics Laboratory, University of Washington, Seattle, Washington

4 March 1993 and 19 November 1993

ABSTRACT

A practical method for determining the CTD thermal-lag correction amplitude α and time constant τ is presented. The method is based upon minimizing the salinity separation of temperature–salinity curves from upcasts and downcasts of a yo-yo sequence of CTD profiles. For the Sea-Bird 9 CTD operated at the 1989 Coordinated Eastern Arctic Experiment O Camp with a 1.75 m s^{-1} water velocity through the conductivity cell, the optimum coefficients are $\alpha = 0.0245$ and $\tau = 9.5$ s. These results combined with those of Lueck and Picklo and results obtained from other Sea-Bird CTDs operating at lower flow rates confirm the flow dependence of α and τ predicted by Lueck but indicate that the theoretical constants are too high. Based on the empirical results, the formulas for α and τ as a function of the average velocity V through the cell are found to be $\alpha = 0.0264V^{-1} + 0.0135$ and $\tau = 2.7858V^{-1/2} + 7.1499$, where V is in units of meters per second.

1. Introduction

A number of sensor mismatch problems come to light in processing conductivity–temperature–depth (CTD) data. The problems of short-term mismatch between the time constants of temperature and conductivity sensors are well known. Recently, another mismatch problem has begun to gain attention. This is the thermal lag of the conductivity sensor due to heat stored in the body of the sensor. If a CTD moves from hot to cold water, for example, heat stored in the body of the conductivity sensor diffuses into the water being sampled and heats it slightly above the temperature of the surrounding water. This raises the measured conductivity above the free-stream value. If the free-stream temperature is used with the sampled conductivity, the derived salinity will be too high. The characteristic timescale of the thermal-lag error can be long compared with short-term mismatch problems. As a result, thermal-lag errors can be difficult to detect; they typically do not stand out as sharp spikes that are obviously wrong. The problem can appear clearly in high-frequency yo-yo CTD data gathered in a thermocline if both down and up casts are examined. Figure 1 shows such a dataset gathered under pack ice at the Coordinated Eastern Arctic Experiment (CEAREX) O Camp, 82.4°N, 6°E, 24 April 1989. In this case a Sea-Bird SBE-9 CTD unit was used with pumped, ducted sensors arranged to allow sampling on upcasts as well as downcasts. Because of the stable platform provided by the ice, the measurements are unaffected by fluctuations in the vertical velocity of the instrument. This makes them ideal for determining the thermal-lag coefficients. The profiles in Fig. 1 are from raw data and display small-scale spikes typical of short-term sensor mismatch. The larger-scale differences between the up and down casts are of special interest here. The upcast curves appear bowed upward and the downcast curves appear bowed downward. The vertical separation between the isopycnals for the upcasts and the downcasts reaches as much as 5 db. This effect does not appear in temperature profiles and does not affect the location of sharp density interfaces. This bowing of the profiles is due to the thermal-lag problem; temperature increase with depth in this location, so a slight positive salini

* Current affiliation: College of Oceanic and Atmospheric Sciences, Oregon State University, Corvallis, Oregon.

Corresponding author address: Dr. James H. Morison, Applied Physics Laboratory, University of Washington, 1013 N.E. 40th Street, Seattle, WA 98105.

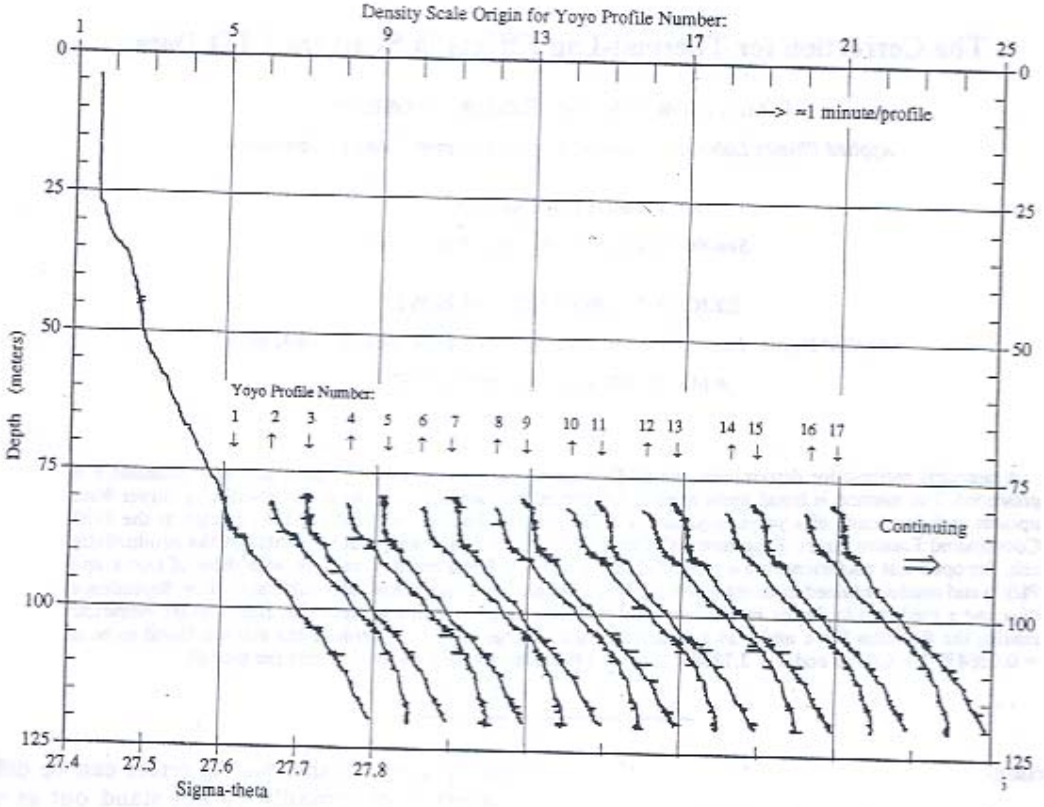

FIG. 1. Yo-yo CTD data gathered under pack ice at the Coordinated Eastern Arctic Experiment (CEAREX) O Camp, 82.4°N, 6°E, on 24 April 1989.

(and density) error occurs on the upcasts going from warm to cold water and a negative error occurs on the downcasts going from cold to warm water.

Lueck (1990) has examined the theory of the thermal-lag problem in detail and has shown that the response of measured conductivity to a step change in temperature of unit magnitude is

$$C(t) = \gamma(1 - \alpha e^{-\beta t})u(t), \tag{1}$$

where γ is the sensitivity of conductivity to temperature, $\partial C/\partial t|_{s,p}$; α is the magnitude of the error; β^{-1} is equal to the time constant τ of the error; and $u(t)$ is the unit step function. Lueck and Picklo (1990) have applied this result to a Sea-Bird CTD unit mounted in a towed profiling device. They develop a correction for the error, C_T, which uses a discrete time domain, recursive filter scheme given by

$$C_T(n) = -bC_T(n-1) + \gamma a[T(n) - T(n-1)]. \tag{2}$$

Here, T is the measured temperature corrected for short-timescale errors, and n is the sample index. Here, C_T is added to the measured conductivity to obtain an estimate of the true free-stream conductivity. Coefficients a and b are related to α and τ by

$$a = 4f_n\alpha\beta^{-1}(1 + 4f_n\beta^{-1})^{-1}, \tag{3}$$

and

$$b = 1 - 2a\alpha^{-1}, \tag{4}$$

where f_n is the sample Nyquist frequency (12 Hz in our data).

In general, the important problem is how to determine the coefficients α and τ for a particular CTD. Lueck and Picklo (1990) determine the coefficients for a pumped Sea-Bird CTD mounted in a towed profiler. They compare the temperature and conductivity responses obtained as the instrument was towed along a slanted path up and down through large thermohaline steps. The steps were about 30 m thick, and the towed body took more than 2 min to move vertically through them: thus it is possible to estimate the coefficients by careful comparison of the step responses of the temperature (which has no thermal lag) and the conductivity sensors, the structure of the resulting salinity

profile, and the gravitational stability of the computed density profile. They find $\alpha = 0.028$ and $\tau = 1/\beta = 9$ s. The arrangement of the steps and the relatively slow speed with which the CTD moved through them made this a viable approach. In most applications, a CTD is used in vertical profiling, and usually the vertical speed is higher than that of the Lueck and Picklo (1990) instrument. In these cases, their technique for determining the coefficients may not be suitable. During CEAREX, the steps were weaker and the CTD moved through them relatively quickly so another analysis approach is needed. This note describes the method for determining the coefficients for the CEAREX O Camp CTD data. We feel the approach might be useful for others with vertical profile CTD data. A description of the CTD system and the other processing steps leading to the thermal-lag derivation is given for completeness. Many investigators may need thermal-lag coefficients for historical archived data or may not be able to perform the yo-yo CTD casts needed to use the method described here. With this in mind we compare the CEAREX O Camp results with determinations of α and τ from other experiments using Sea-Bird sensors, and derive empirical expressions for α and τ as functions of the average velocity through the conductivity cell. These expressions should help others choose reasonable, first-order values for the coefficients in the absence of other data.

2. The CTD system

The CTD instrument used in CEAREX is shown in Fig. 2. It is a Sea-Bird SBE-9 equipped with identical primary and secondary pairs of SBE-3 temperature (serial numbers 905 primary and 602 secondary) and SBE-4 conductivity (serial numbers 558 primary and 553 secondary) sensors and a Paroscientific pressure sensor. Each pair of conductivity–temperature sensors is mounted horizontally, with the thermistor 12 cm away from the side of the main pressure case. The sensors are connected by plastic ducts as shown in Fig. 2. These are fitted over the thermistor and plumbed into one end of the conductivity cell. A single SBE-5 pump is connected to the other end of each conductivity cell with a Y tubing arrangement. The pump draws water past the thermistors and through the conductivity cells. With this arrangement, water is sampled as far as possible outside the turbulent wake of the instrument and is uncontaminated by the thermal mass of the CTD housing on both upcasts and downcasts. Laboratory tests of this specific pump and plumbing system indicate the flow rate through the pump is 0.044 L s^{-1} total, or 0.022 L s^{-1}, for each sensor pair. Inside the 4-mm-diameter conductivity cell, this results in an average velocity of 1.75 m s^{-1}.

A Sea-Bird SBE-11 deck unit and a Macintosh II computer were used to operate the CTD and record the data. The Sea-Bird SEASOFT, MS-DOS-based, data acquisition software was modified to run on the Macintosh computer. All CTD channels were recorded at 24 Hz, which corresponds to a depth sampling interval less than 4 cm for all lowering speeds used during CEAREX. The computer also controlled the winch, driving the dc electric motor through a National Instruments NB-AO-6 digital-to-analog converter and a Danfoss A2000 motor controller. With this system the CTD can be left to cycle unattended for hours at a time with little variation in speed or cycle time (Andersen and Morison 1989).

3. Basic processing for short-term mismatch

Before deriving and applying the thermal-lag corrections, it is necessary to correct the signals for short-term mismatch of the sensor responses that produce salinity spikes. The problem of salinity spiking has been dealt with in detail by Bray (1987), Gregg and Hess (1985), Gregg et al. (1982), Horne and Toole (1980), and Ochoa (1989). Larson (1989) gives directions for applying the appropriate corrections for pressure sensor dither, temporal alignment of the temperature and conductivity measurements, and time response mismatch between the temperature and conductivity sensors. We have added a correction for temporal misalignment of the pressure measurement with the temperature and conductivity measurements. Although this correction is short term, it is made after, and is related to, the thermal-lag correction. Therefore, it is discussed in the thermal-lag section. Figure 3 is a block diagram of the basic steps used here to determine and apply corrections for short-term mismatch of sensor response.

The first step in Fig. 3 is the filtering of pressure. The pressure sensor dither is caused by least-count chatter and fluctuations in dynamic pressure due to turbulent variations in water velocity around the pressure port. When working with high-frequency data, this dither can be a significant fraction of the distance the CTD moves between samples. A program called SmoothP for the Macintosh computer has been adapted from code originally developed by Sea-Bird Electronics, and is used to make the correction. It smoothes the depth record by applying a symmetric, 15-scan (0.625 s), triangular-weighted filter to the pressure channel. Figure 4 shows a down–up pair of raw temperature and salinity profiles with smoothed pressure corresponding to the first pair of Fig. 1.

The heart of the short-term mismatch problem is correcting for differences in time response and alignment. For our purposes, the time responses can be approximated by e-folding time constants. The conductivity cell time constant is related to the time required for water to flush the active volume of the cell. Thus, it is a function of cell volume, flow rate, and, because

1.75 m/s

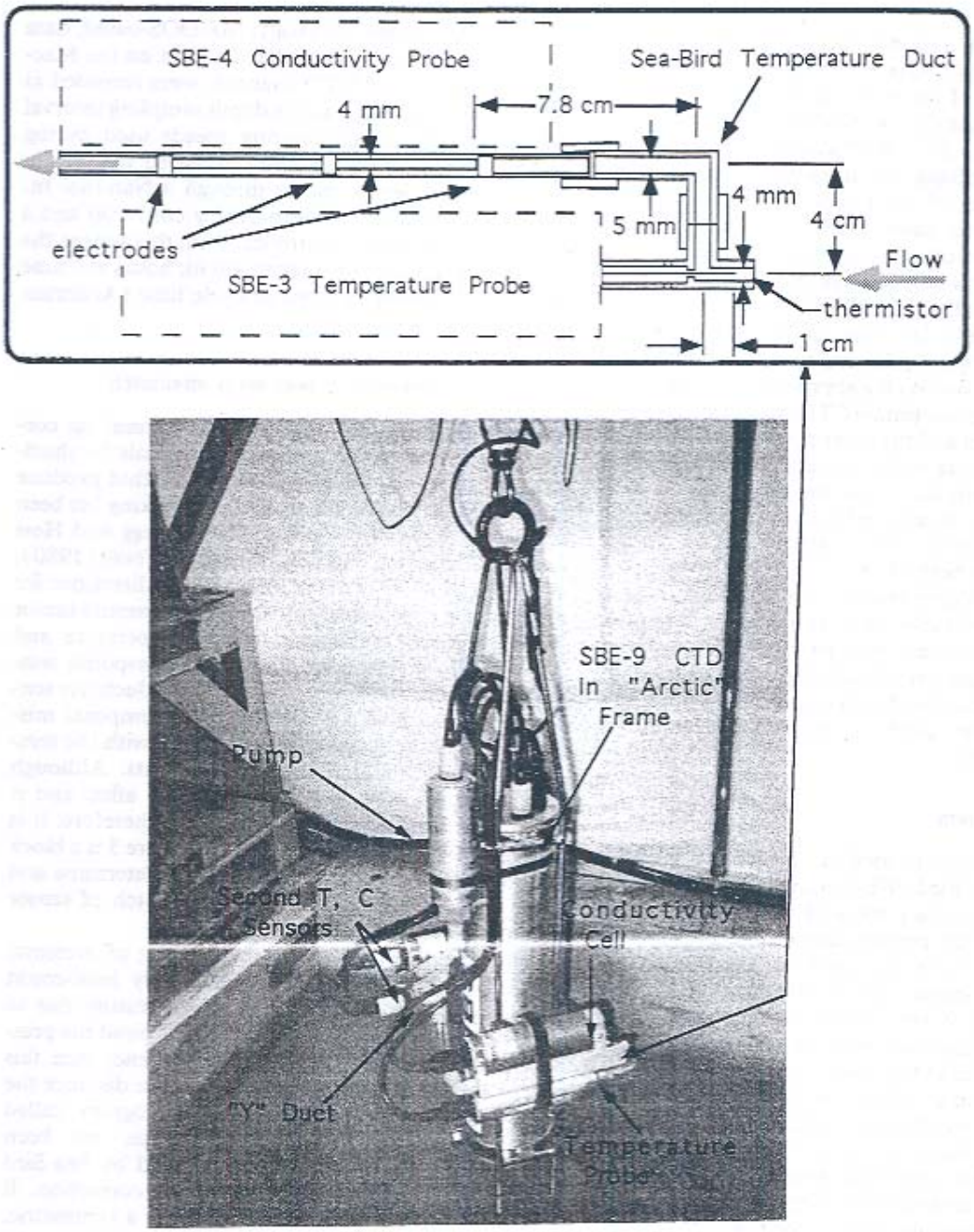

FIG. 2. The CTD instrument used in CEAREX. The horizontally mounted, ducted probes and the pump are shown. The duct geometry is shown in the inset.

of boundary layer effects, the geometry of the upstream plumbing. For a conductivity cell used with a temperature sensor duct, the time constant is 0.082 s at a flow rate of 0.022 L s^{-1}. The temperature sensor has a time constant of about 0.07 s at 0.022 L s^{-1} (1.75 m s^{-1}) and may vary slightly with flow rate. For the Sea-Bird duct system, flow rate is fixed by the pump, so the temperature and conductivity time constants are independent of the speed of the CTD.

Temporal misalignment is due primarily to the fact that the temperature sensor is upstream of the conductivity sensors. The lag of conductivity due to down-

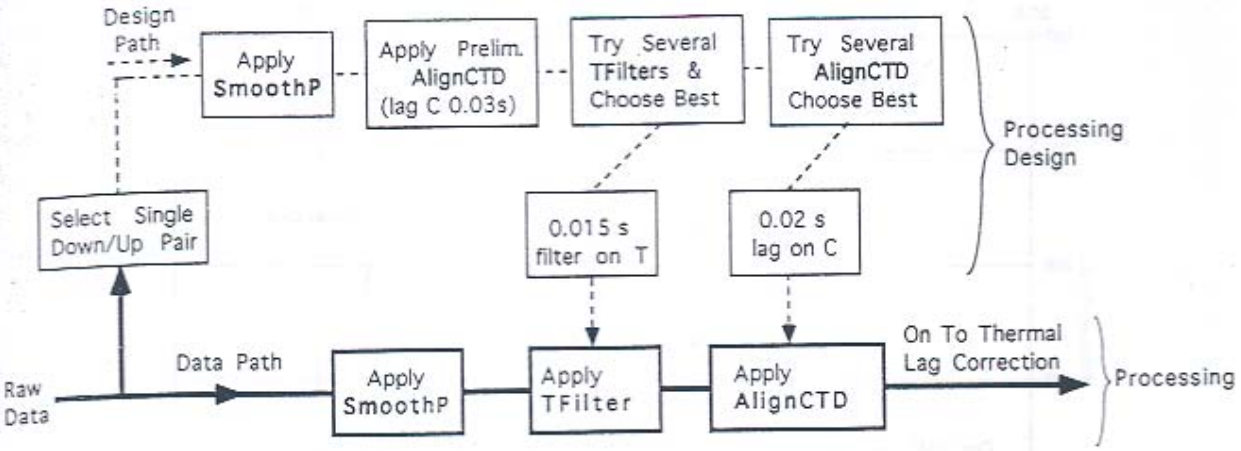

FIG. 3. Block diagram of the basic steps used to determine and apply corrections for short-term mismatch of sensor response.

stream position is anticipated by the manufacturer, and a three-scan (0.125 s) advance is applied to the conductivity signal by the firmware of the CTD deck unit during recording. For most applications, including this one, this puts temperature and conductivity in approximate alignment, but some adjustment for individual instruments is still required during processing.

To a lesser degree, the difference in time response is also a source of misalignment. Therefore, the corrections for misalignment and time response are derived in an iterative fashion. First, data from a profile through a region of very sharp gradients are chosen. These data are usually processed for a series of temporal shifts of conductivity relative to temperature. For the optimum time shift, the salinity spikes occur as symmetric positive and negative pairs and are a minimum in size. This indicates that the temperature and conductivity measurements are coordinated to the same parcel of

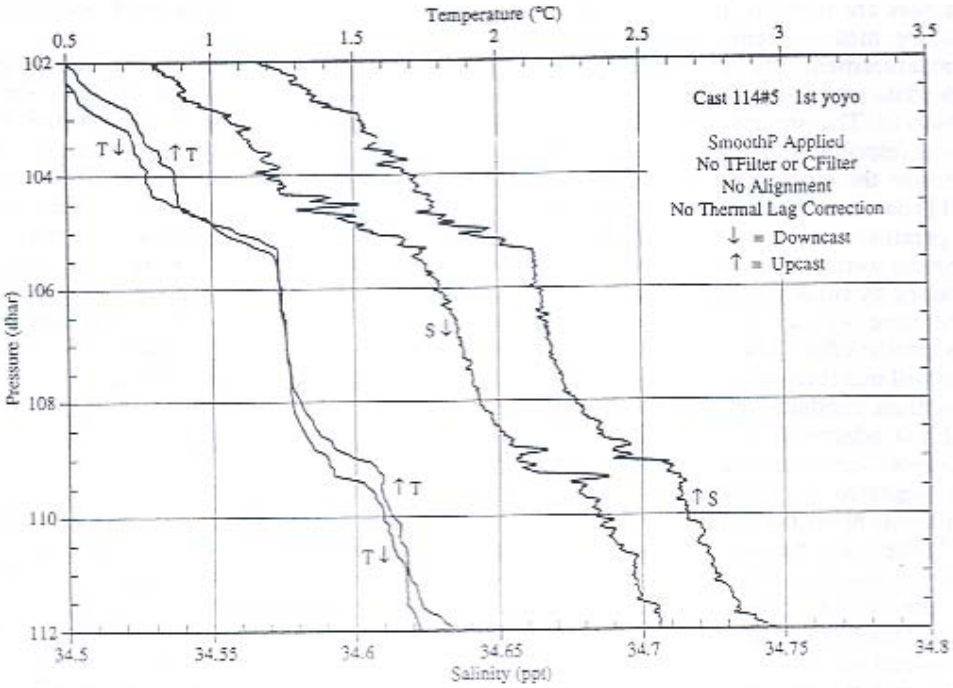

FIG. 4. A down-up pair of raw temperature and salinity profiles from the first down-up pair of the high-frequency yo-yo section shown in Fig. 1.

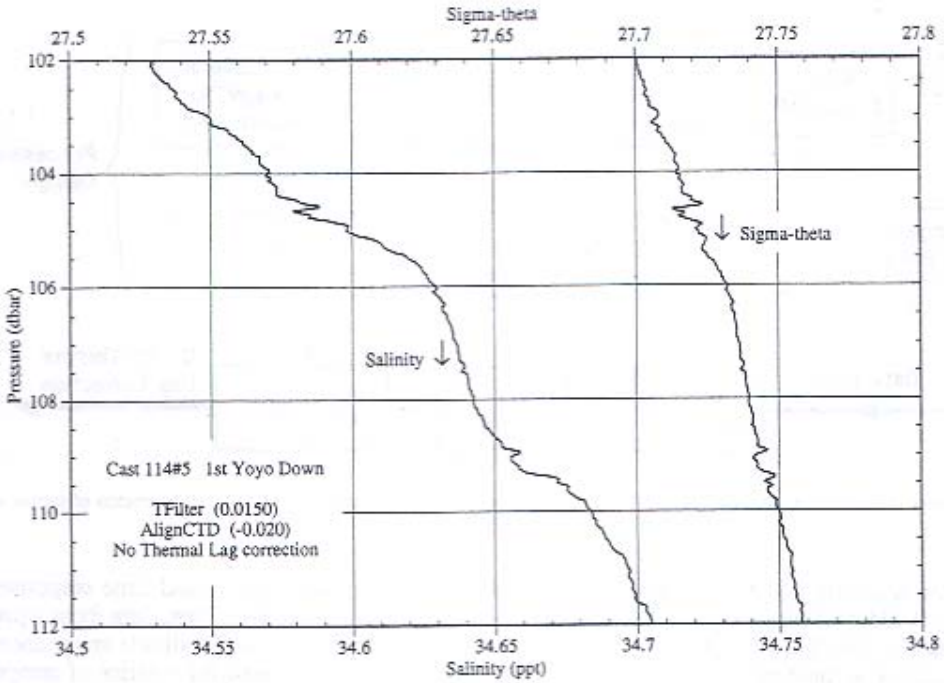

FIG. 5. The data of Fig. 4 after applying the 0.015-s temperature filter and a 0.02-s conductivity lag.

water in the conductivity cell. The remaining symmetrical spiking is due mainly to mismatch of the temperature and conductivity measurements. The symmetric spikes are reduced in size by filtering the faster-responding measurement to match the slower-responding measurement. The filter choice is made by processing the data with various filters until minimum spiking is observed. The process of selecting alignment time shifts and response matching filters may be iterated to determine the optimum combination.

For the CTD data used here, initial analysis was done for both temperature–conductivity sensor pairs, but the secondary sensors were, for some unknown reason, less subject to fouling by small pieces of floating biological material. Therefore, we used the secondary pair for the bulk of the scientific effort. The secondary sensors also seemed fairly well matched, with the temperature being slightly faster than conductivity. We used a program called AlignCTD, adapted to the Macintosh from Sea-Bird code, to apply various conductivity lag times. This initial effort suggested a 0.03-s conductivity lag. We then tried different filters on temperature using a program called TFilter (also adapted from Sea-Bird code). This is a one-pole low-pass filter run forward and then backward to prevent any phase shift. As shown in the upper portion of the block diagram of Fig. 3, we applied TFilter with several values of time constant to the down cast of Fig. 4 adjusted with the 0.03-s conductivity lag. A 0.015-s filter reduced the large salinity spikes the most at 105 and 109 db and generally produced the smoothest profiles. That the filter time constant is so short merely indicates the temperature and conductivity sensor response times were nearly equal to begin with.

In a final iteration, we applied AlignCTD with various conductivity lags to the data with the 0.015-s temperature filter. Figure 5 shows the data from the downcast of Fig. 4 with the optimum combination: a 0.015-s temperature filter and a 0.02-s conductivity lag. The density spikes near 105 db were biased positive for a 0.01-s lag and negative for a 0.03-s lag, but are symmetric for the 0.02-s lag. The magnitude of the smaller high-frequency spikes is also minimum for this lag. The 0.015-s temperature filter and 0.02-s lag correction are in addition to the 0.125-s conductivity advance applied during recording.

4. Thermal-lag correction

The conductivity correction proposed by Lueck and Picklo (1990) modifies the measured conductivity according to (2). This recursive correction is a function [(3) and (4)] of α, the initial amplitude of the temperature error for a unit step change in ambient temperature, and $\tau = \beta^{-1}$, the e-folding time of the temperature error. The problem is to determine the correct values of α and τ for a particular CTD. The technique used here is to compare the temperature–salinity (T–

S) diagrams for down- and upcasts when using different values of α and τ. It is based on the assumption that the T–S relationship does not change between the down- and upcast. The correct values of α and τ produce the least separation between the down- and upcast T–S curves. For example, Fig. 6 shows T versus S for the downcast and subsequent upcast corresponding to Fig. 5. The total separation is about 0.04 psu, for a thermal-lag error on each cast of 0.02 psu. As also indicated by the figure, we found by trial and error that the T–S plots pull together if the thermal-lag correction [(2), (3), and (4)] is applied with $\alpha = 0.0235$ and $\tau = 11.0$ s.

Lueck and Picklo (1990) report that the effect of an error with a 10-s time constant can be detected for up to 45 s. As a result, a single 2-min down–up pair probably does not provide enough data for a robust estimate of α and τ. More representative estimates of α and τ were obtained using the method illustrated in Fig. 7 with 31 down–up pairs of a 39-pair, 2-h yo-yo sequence. Eight pairs were not used because of transient biological contamination. The method involves first processing the data with 273 combinations of α and τ ranging from $0.0185 < \alpha < 0.0285$ and $7 < \tau < 13$. For each α, τ combination, the downcast data are separated into 0.05°C temperature bins, and the average salinity in each bin is computed. The same is done for the processed data from the upcasts. The down–up separation in T–S space is then computed as the average, over all temperature bins, of the absolute value of the difference between downcast and upcast salinity in each bin.

Processing the full yo-yo sequence 273 times proved time consuming. To do this as efficiently as possible, we changed the way the thermal-lag correction is applied. In the scheme of Lueck and Picklo (1990), the conductivity is corrected using (2). In reality, the thermal lag is not a conductivity error, but a temperature error. The raw conductivity readings are a true measure of the conductivity in the cell, but the temperature in the cell is not equal to the measured free-stream temperature. Here, rather than correct conductivity to the value outside the cell, we compute the temperature inside the cell for the sole purpose of calculating salinity. The temperature version of (2) is

$$T_T(n) = -bT_T(n-1) + a[T(n) - T(n-1)]. \quad (5)$$

Here, T_T is the temperature correction that is subtracted from the measured ambient temperature to estimate the temperature in the conductivity cell, T is the filtered and aligned measured temperature, and n is the sample index. This approach is more direct and saves at least some computational effort because it is unnecessary to compute the sensitivity of conductivity to temperature, γ, used in (2). Using the scheme of Lueck and Picklo (1990), γ must either be estimated for some range of temperature and salinity or, in a worst case, computed for each point. Computing γ is an iterative process and involves several computations of conductivity and sa-

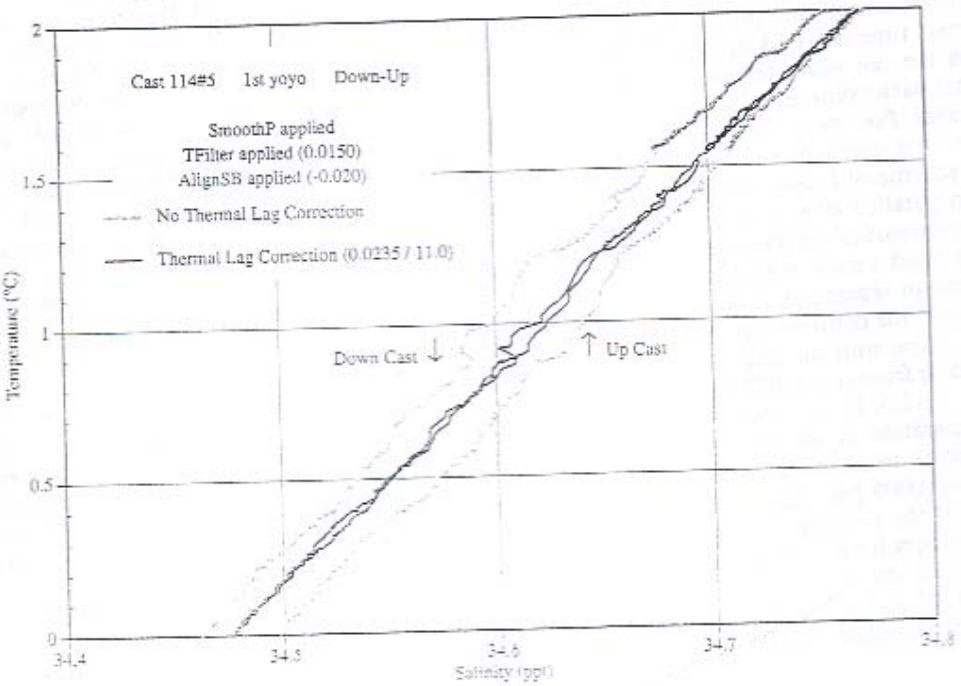

FIG. 6. Temperature vs salinity for the downcast and subsequent upcast corresponding to Fig. 5. The T–S plots for $\alpha = 0.0235$ and $\tau = 11.0$ s are also shown.

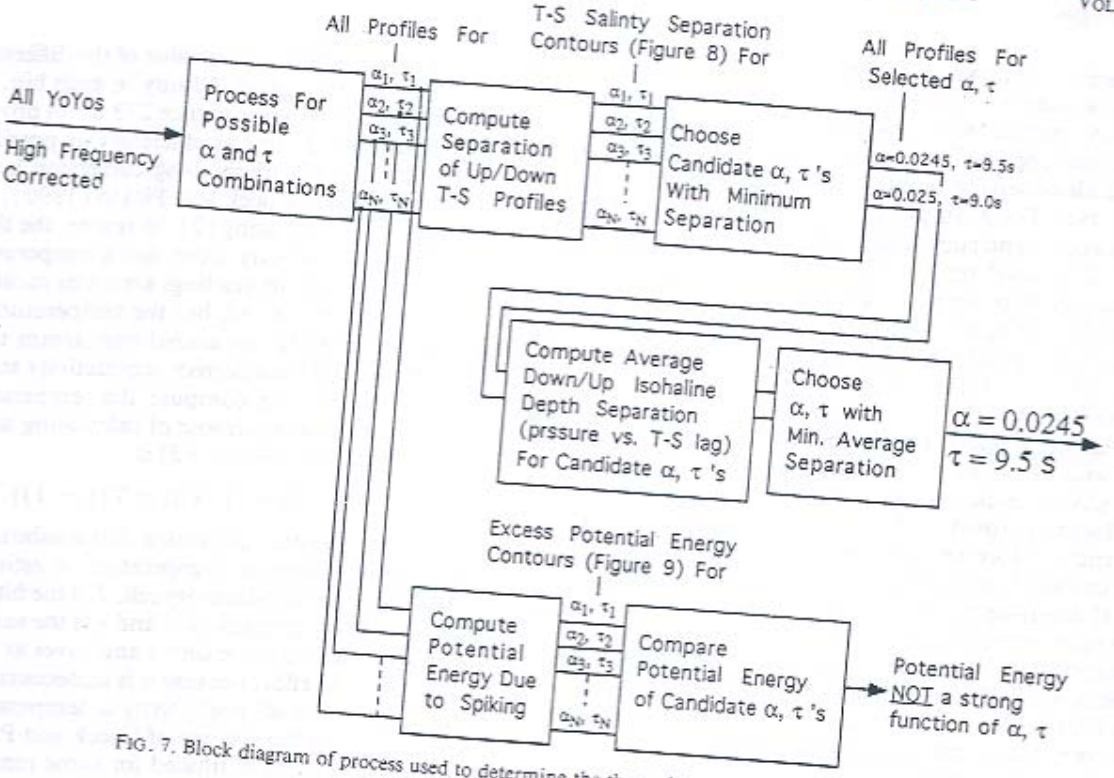

FIG. 7. Block diagram of process used to determine the thermal-lag correction coefficients.

linity. With this scheme, corrected cell temperature is computed and used solely, along with measured conductivity, to calculate salinity at every time step. Density is calculated from salinity and the measured ocean temperature at every time step and all three are stored. Conductivity and the cell water temperature are not retained so the net data volume does not increase as processing progresses. For the O Camp data, the new scheme runs about six times faster than our implementation of the scheme of Lueck and Picklo (1990) using (2) with computation of γ at every point.

Figure 8 shows contours of the average, absolute salinity separation plotted versus α and $\tau = \beta^{-1}$. The region of the minimum separation is obviously not a single point. However, the contours do show a closed, curved, troughlike shape with the axis of the bottom of the trough extending from $\alpha = 0.0285$ and $\tau = 7.5$ s to $\alpha = 0.021$ and $\tau = 12.5$. In the trough the average, absolute salinity separation is less than 0.0011. The white contours indicate small, isolated minima with separations less than 0.0009 psu. Their rather angular shape is an artifact of the plotting routine. The very smallest separation occurs for $\alpha = 0.025$ and $\tau = 9$ s, but the widest region of the bottom of the trough is centered on $\alpha = 0.0245$ and $\tau = 9.5$ s. The average absolute separation is less than 0.0009 psu at these values.

The vertical profiles were also examined for changes in the amount of density inversion associated with the different combinations of α and τ, a physical benchmark similar to that used by Lueck and Picklo (1990). This was done in an objective way by computing the average excess potential energy for density profiles produced with each α, τ combination. The excess potential energy is the difference between the potential energy of the water column as computed from the CTD density profile and the potential energy computed after sorting the profile by density with the most dense water on the bottom. Spikes result in density inversions that raise the excess potential energy. It was thought that this might add an independent criterion for choosing between α, τ pairs.

Figure 9 shows the contours of excess potential energy versus α and τ. Unlike Fig. 8, the contours of excess potential energy show no distinct minimum, but rather a slight decrease with increasing τ. This is because, for the rapidly moving O Camp CTD, density inversions occur only over short depth scales and timescales. The thermal-lag corrections have no effect over such short timescales. Thus, for this situation, density inversions are not good indicators for selecting the thermal-lag coefficients, although it does suggest that if all else is equal, larger values of τ are better.

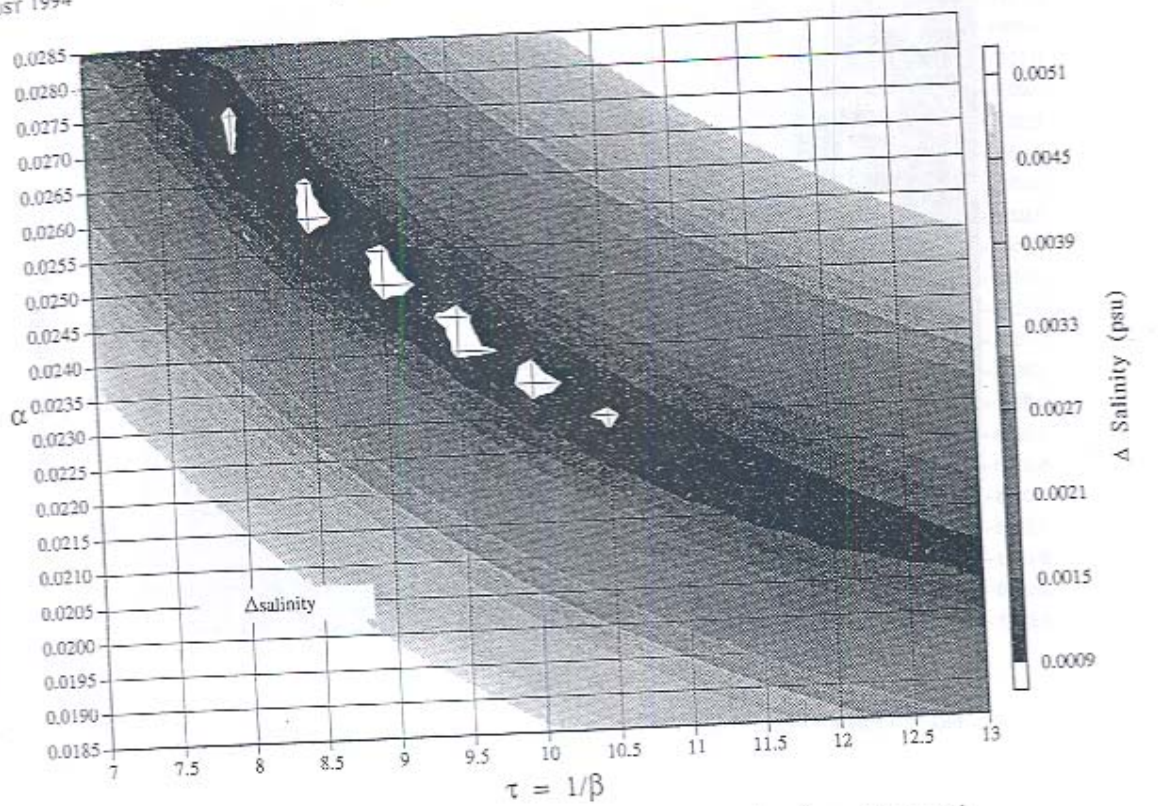

FIG. 8. Contours of the average absolute salinity separation plotted vs α and $\tau = \beta^{-1}$.

Our final choices for α and τ are $\alpha = 0.0245$ and $\tau = 9.5$ s. These values were chosen over those producing the absolute minimum separation in Fig. 8 for three reasons. First, they are at the center of the bottom of the trough and the trough is widest there. This should reduce the sensitivity of the correction to variations in parameters controlling the thermal-lag error. Second, excess potential energy is slightly less at $\alpha = 0.0245$ and $\tau = 9.5$ s than at $\alpha = 0.0250$ and $\tau = 9.0$ s. Finally, as discussed below, the net lag in the temperature and salinity readings is slightly less at $\alpha = 0.0245$ and $\tau = 9.5$ s than at $\alpha = 0.0250$ and $\tau = 9.0$ s, suggesting less degradation of the overall speed of response.

The alignment of the pressure signal with the temperature and conductivity signals can be tested by comparing isopycnal depths measured on upcasts and downcasts over the short yo-yo sequence. For this analysis, the cycle frequency should be greater than the local Brunt–Väisälä frequency, and for these data, it is an order of magnitude greater. Figure 10 shows isohaline depths for all the up- and downcasts processed with $\alpha = 0.0245$ and $\tau = 9.5$ s. The isohaline depths display offsets between successive down- and upcasts, resulting in a high-frequency sawtooth pattern. The variations are exaggerated between 80 and 90 db and near 100 db three-fourths of the way through the record. The presence of unstratified layers in these areas results in large shifts due to very small errors in density. In the areas with appreciable stratification, the sawtooth variations are up to 0.5 db, and are due to pressure misalignment. On average, the isohalines from upcasts are 0.21 db higher than those from downcasts in the stratified areas, indicating the temperature and salinity measurements lag the pressure measurement by 0.105 db. This corresponds to 0.157 s, or about four scans. The lag can be accounted for by a combination of the approximately 0.080-s response delay of the temperature and conductivity measurements on water entering the duct and a comparable delay due to deflection of the T–S structure by the moving CTD. Such slight deflection has been observed subjectively ahead of moving instruments in laboratory tests. In this case the deflection corresponding to a 0.08-s delay is 0.05 db. To correct the problem, the pressure data is lagged four scans relative to temperature and salinity. Figure 11 shows isohaline plots after lagging the pressure data of Fig. 10 by four scans. Most of the sawtooth pattern is gone in the stratified areas, and the variations are more random in most of the unstratified areas.

The pressure alignment was also performed for data processed with $\alpha = 0.025$ and $\tau = 9.0$ s and with α

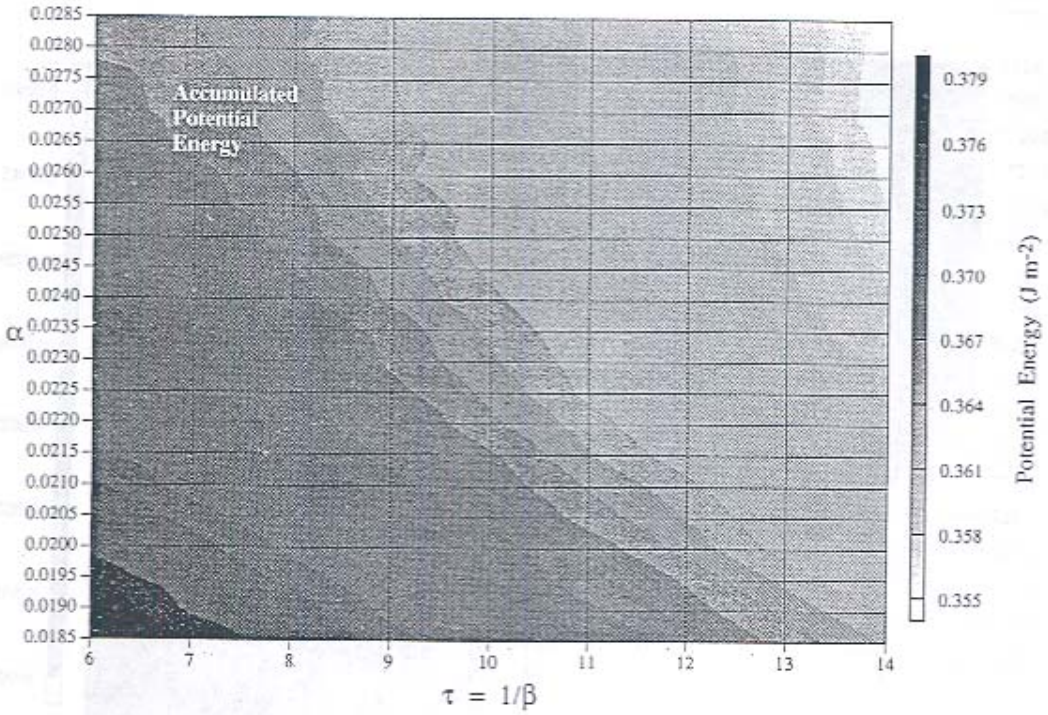

FIG. 9. Contours of excess potential energy (J m^{-2}) over 31 yo-yo pairs vs α and $\tau = \beta^{-1}$.

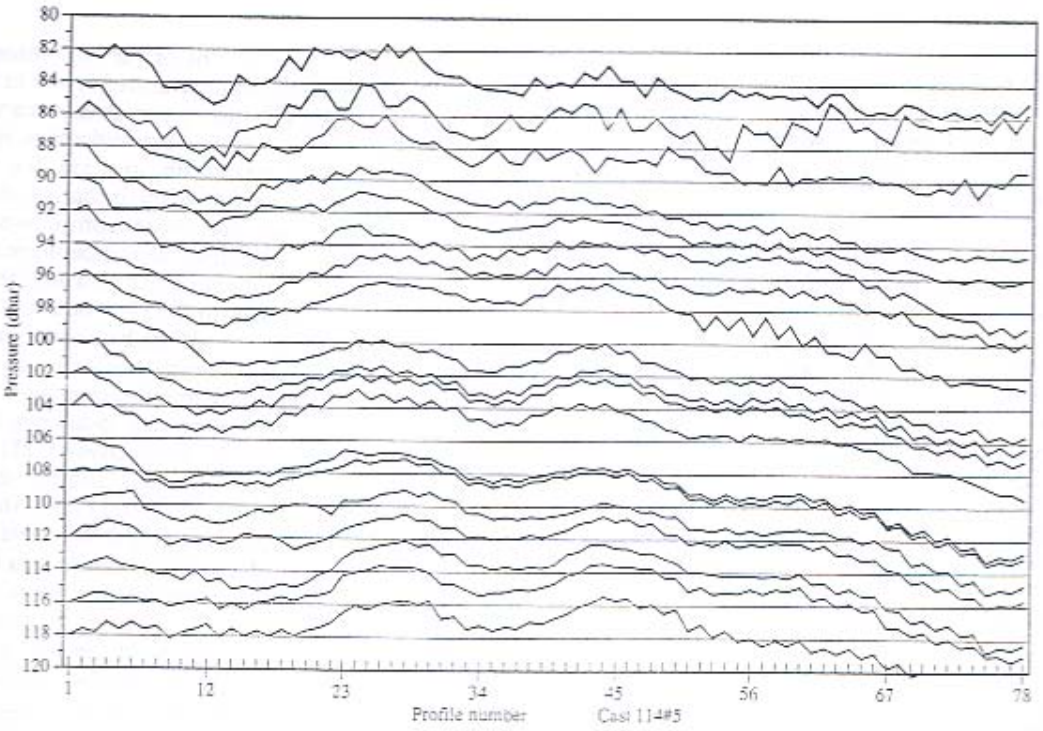

FIG. 10. Isohaline depths from all the up- and downcasts processed with $\alpha = 0.245$ and $\beta = 9.5$.

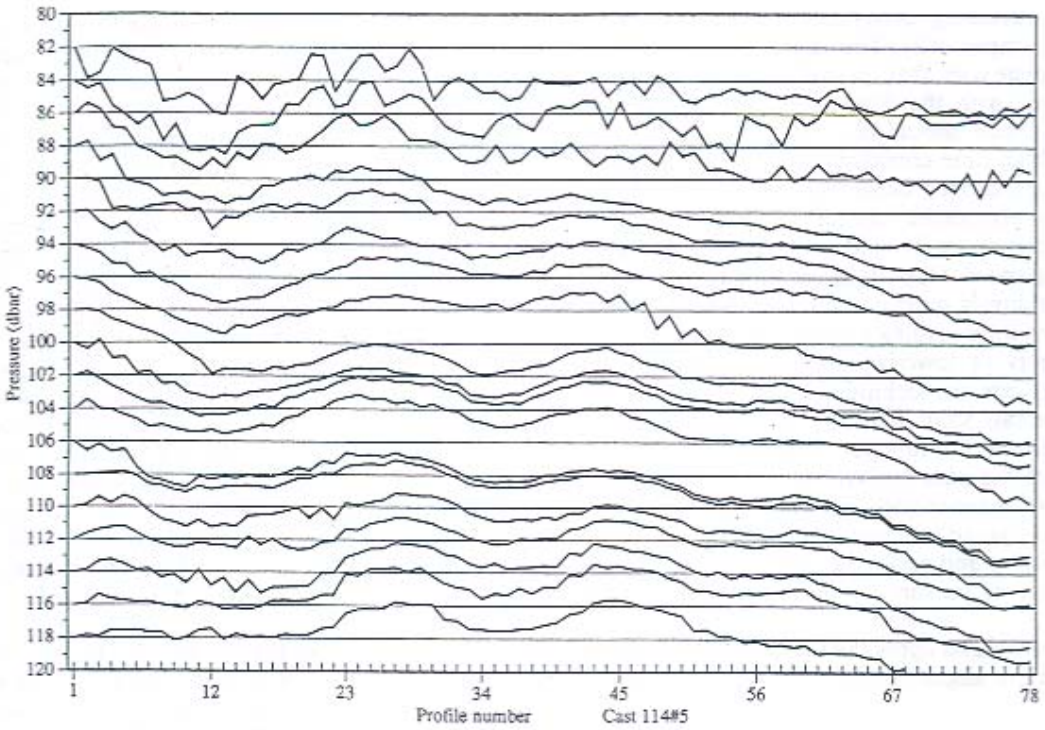

FIG. 11. Isohaline plots for $\alpha = 0.0245$ and $\tau = 9.5$ after lagging the pressure data of Fig. 11 by four scans.

$= 0.0235$ and $\tau = 10.0$ s. The results both required slightly larger pressure alignment corrections suggesting slightly larger aggregate sensor response delay. This was an added factor favoring the final choice of $\alpha = 0.245$ and $\tau = 9.5$ s.

5. Summary, recommendations, and comparison with other results

The processing described here made substantial improvements in the O Camp CTD data quality. The initial processing for short-term mismatch reduced the salinity spiking at the 0.1–0.5-m depth scale by a factor of about 5. Figure 4 shows that in the unprocessed data, spikes of about 0.005 psu were common at the 0.10–0.20 depth scale and there are a couple of 0.01–0.02 spikes at the 0.5-m scale. Figure 5 shows that the numerous small spikes are reduced to less than 0.001 psu and the large spikes are reduced to less than 0.004 psu. The thermal-lag problem persists over a much larger depth scale; Fig. 1 suggests tens of meters. In T–S space (Fig. 6) the typical average separation between raw upcast and downcast profiles is 0.04 psu indicating an unprocessed salinity error of 0.02 psu in the thermocline. After the thermal-lag processing, the average absolute separation is less than 0.0009 psu (Fig. 8). The pressure correction suggests the net lag of temperature and conductivity is 0.157 s. This is due to the time response delay of the sensors and disturbance of the water by the moving CTD.

The method described here for determining the thermal-lag coefficients and applying the corrections was based on the fact that the CTD was being used to gather up- and downcast yo-yo data. However, the techniques might be used in any CTD program if a few key steps are taken.

1) Configure the CTD sensors such that they produce useful data on upcasts as well as downcasts. With the Sea-Bird SBE-9, this means use a pumped, ducted pair of temperature–conductivity sensors. The sensors should be positioned away from the body of the CTD and oriented so as to sample undisturbed water going down and up (e.g., sensors horizontal and sticking out). For CTDs being operated in a yo-yo manner, these are probably wise steps in any event. For CTDs being used for deep casts with rosette bottles, it may be appropriate to arrange the sensors differently for the test casts. For a pumped Sea-Bird cell, keep the length of the tubing the same and follow the manufacturer's recommendations for avoiding dynamic pressure and inertia effects. The goal is to produce, in the test case, flow conditions through and around the conductivity cell as near to those of the routine casts as possible, while allowing good sampling both going up and down.

2) Go to sea and find a region with a strong temperature gradient. Perform yo-yo CTD casts at the

normal operating speed (the speed is not so important with a pumped cell). The casts should be done over a depth range such that the down–up cycle time is short compared with the Brunt–Väisälä period. However, the cycle time should be substantially larger than the thermal-lag time constant; 2–5 min per cycle is sufficient. In the open ocean the advantage of the stable platform provided by the ice may be lost. Ship motion may cause variation and even reversals in the CTD lowering speed. Opportunities should be sought to do the tests during quiet conditions if possible. However, assuming the pumping system is plumbed to minimize the effects of lowering speed and acceleration on pumping rate, the technique should work even if heave and reversals occur. This is so because the thermal-lag phenomenon is a function of time, and the technique examines the data in T–S space without reference to depth. A heave-induced reversal should appear as a very short yo-yo segment.

3) Derive and apply the corrections for short-term mismatch of sensors by following the flowchart in Fig. 3.

4) Derive and apply the thermal-lag correction and the pressure alignment by following the flowchart in Fig. 7.

But how should the thermal-lag problem be handled if the CTD data were gathered in the past or if they were gathered with a Sea-Bird conductivity cell used in an unusual application? The key variable determining α and τ is the average velocity V of the water through the cell. According to Lueck's (1990) arguments, α should vary as V^{-1} and τ should vary as $V^{-1/2}$. An empirical relationship between α and τ can be estimated from the results for several different CTDs. Lueck and Picklo (1990) examine the performance of a particular pumped Sea-Bird CTD application in a towed body; here we have determined α and $\tau = \beta^{-1}$ for a fairly standard, pumped, ducted temperature, CTD application. It is difficult to extrapolate the analysis of these two systems to other cases because, in spite of the differences in application, the flow velocity through the cells is not that different. For the Lueck and Picklo (1990) application, the velocity is estimated to be 2.4 m s^{-1}; here it is 1.75 m s^{-1}. The values of α and τ are also similar. To put these results into perspective, we must look at the results for an additional instrument system.

As another component of CEAREX, two of the authors (D'Asaro and Boyd) made CTD casts in the area of the West Spitsbergen Current in the winter of 1989 with a loosely tethered, free-fall instrument containing an unpumped SeaCat CTD and Sea-Bird microconductivity cells. The thermal-lag problem manifests itself in the data gathered in large (>20 m) thermohaline steps. The thermal-lag error gives rise to apparent unstable stratification in the large isothermal layers bounded by sharp temperature and salinity gradients. The appropriate α and τ values have been successfully determined using methods similar to the potential energy calculation described here for the O Camp CTD data. The data were analyzed by iterating over a range of α and τ values. The correct values were chosen as those minimizing density inversions. The free-fall probe was used at three different fall rates: 0.36 m s^{-1} (ultraslow), 0.5 m s^{-1} (slow), and 0.96 m s^{-1} (medium). Estimates of the average velocity through the active segment of the cell are needed to compare the results on an equal basis with the other CTD data. We base our estimates on the balance between the head loss of the laminar flow through the cell and the dynamic pressure due to the lowering speed. As pointed out by Lueck (1990) the flow in the cell is not fully developed, so the approach of Hansen (1967) was used to determine the effective friction factor for the undeveloped flow. For a lowering speed of 0.96 m s^{-1} the average cell velocity is 0.41 m s^{-1}, for 0.5 m s^{-1} the cell velocity is 0.17 m s^{-1}, and for 0.36 m s^{-1} the cell velocity is 0.10 m s^{-1}.

The results from the O Camp CTD, the Lueck and Picklo (1990) device, and the free-fall probe are compared in Fig. 12. Figure 12a plots α versus average water velocity, V, through the cell, and Fig. 12b plots τ versus velocity. Theoretical values of α and τ inferred from Lueck's (1990) Table 2 are also shown. Curves of the form $\alpha = aV^{-1} + b$ and $\tau = aV^{-1/2} + b$ are fit to the data. The fit of these equations to both the actual and the theoretical data is good. This argues for the fundamental soundness of Lueck's (1990) theoretical approach. The shape of the theoretical and empirical curves is the same, but the theoretical values of τ are 50% greater than the measured values, and the theoretical α values are about 75% higher. This suggests that the actual rate of heat transfer from the glass of the cell is greater than predicted, and that the internal boundary layer thickness is less than predicted. It is possible that heat loss from the outside of the cell decreases the time constant. However, it is doubtful that this is a major factor, because the amount of such external flushing must be quite different for the various instrument configurations considered here, while the results are very consistent.

Additional values of α for a Sea-Bird CTD are given by Huyer et al. (1993) and Huyer (1993, personal communication). These were determined for a pumped cell mounted in a SEASOAR towed profiler. The values were derived with an assumed value of τ = 10 s by choosing values of α which, upon visual inspection, best closed T–S contours from down and up profiles in the thermocline. The values of α and the best sensor alignment varied due to flow rate variations associated with the hydrodynamics of the SEASOAR and the placement of the CTD intake and exhaust. The average velocity through the cell was estimated

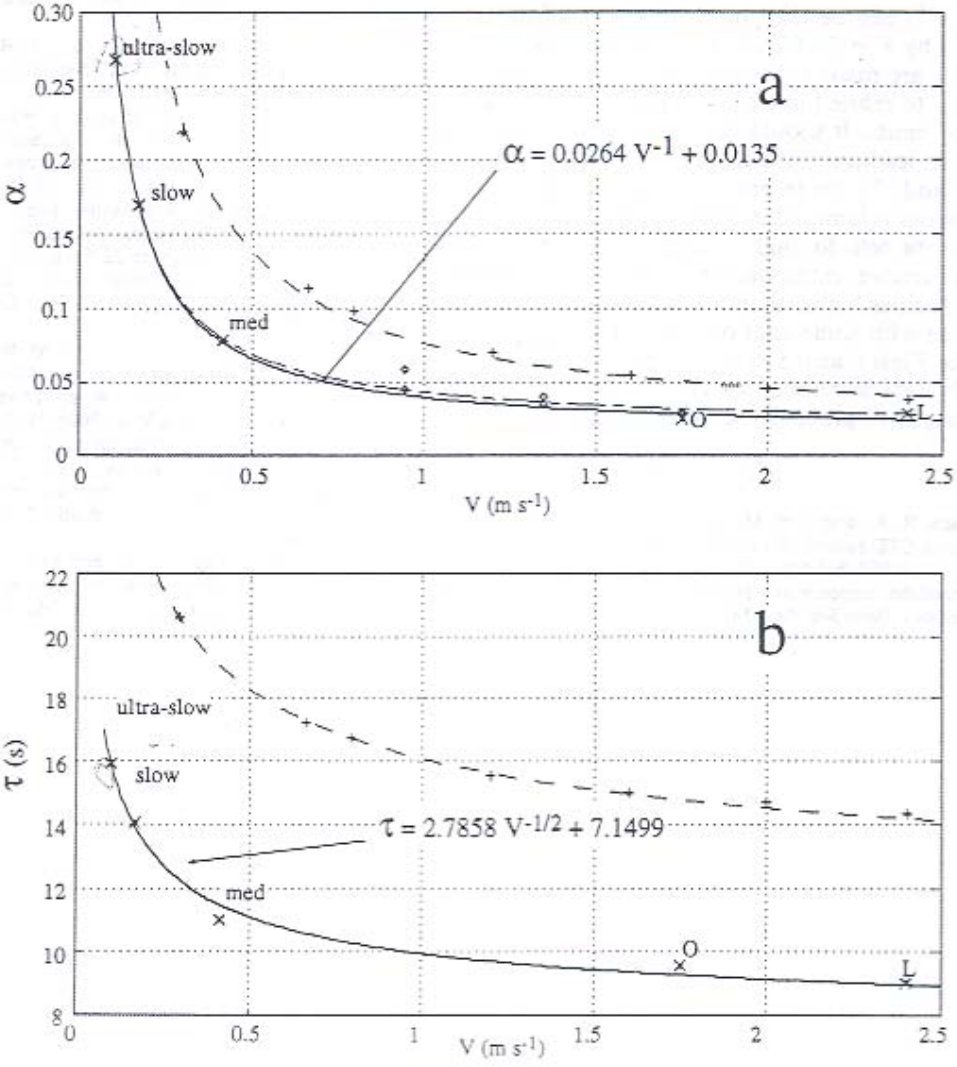

FIG. 12. (a) Curve fit of α to V^{-1}, $\alpha = 0.0264V^{-1} + 0.0135$, for the ultraslow, slow, and medium CEAREX SeaCat data, and the CEAREX O Camp (O) and Lueck (L) data. For ultraslow, slow, and medium, the velocity is calculated from lowering velocity assuming nonequilibrium laminar pipe flow driven by dynamic pressure at the cell inlet. Pluses indicate α inferred from Lueck (1991), Table 2 theory, and the curve fit to theory is $\alpha = 0.0615V^{-1} + 0.0155$. Diamonds denote points from Huyer et al. (1993), and the curve fit (long dash-short dash) with these included is $\alpha = 0.0260V^{-1} + 0.0175$. (b) Curve fit of τ to $V^{-1/2}$, $\tau = 2.7858V^{-1/2} + 7.1499$. Pluses indicated τ inferred from Lueck (1991), Table 2 theory, and the curve fit to theory is $\tau = 5.3348V^{-1/2} + 10.7410$.

based on the observed alignment delay between temperature and conductivity. Values of α at three typical velocities are also shown in Fig. 12a. These data have not been incorporated into our recommended curve fit, in part because of the assumed constant τ value upon which they are based. In fact the assumed value of τ appears to be a fairly good choice and the α data lie nearly on the curve fit derived here. As the figure shows the curve fit incorporating the Huyer et al. (1993) α data is very similar to the one for the O Camp, free-fall probe, and Lueck data.

The agreement of the measurements with the $\alpha \sim V^{-1}$ and $\tau \sim V^{-1/2}$ fits is especially significant considering the variety of instrument applications and analysis techniques. In cases where it is difficult to determine α and τ directly for a Sea-Bird cell, the equations

$$\alpha = 0.0264V^{-1} + 0.0135 \quad (6)$$

and

$$\tau = \beta^{-1} = 2.7858V^{-1/2} + 7.1499 \quad (7)$$

can be used to calculate α and τ if V is known. Here, V (m s^{-1}) can be related to the volume flow rate Q (L s^{-1}) by $V = 79.577Q$. As more determinations of α and τ are made for various situations, it should be possible to refine these equations and determine confidence limits. It should be noted that the scaling arguments leading to the forms of velocity dependence in (6) and (7) rest in part on the assumption that the flow remains laminar. According to Lueck (1990) the flow in the cells for high velocities is not far from critical. Therefore, extrapolation of (6) and (7) to average cell velocities higher than those examined here should be done with some caution. The curves also indicate that for V less than 0.5 m s^{-1}, the performance degrades rapidly with decreasing cell velocity and any coefficient estimates will probably be more uncertain.

REFERENCES

Andersen, R. A., and J. H. Morison, 1989: A computer-controlled yo-yo CTD system for the Arctic. *Proc. Oceans '89*, 1263–1266.

Bray, N. A., 1987: Salinity calculation techniques for separately digitized fast response and platinum resistance CTD temperature sensors. *Deep-Sea Res.*, **34**, 627–632.

Gregg, M. C., and W. C. Hess, 1985: Dynamic response calibration of Sea-Bird temperature and conductivity probes. *J. Atmos. Oceanic Technol.*, **2**, 304–313.

——, J. C. Shedvin, W. C. Hess, and T. B. Meagher, 1982: Dynamic response calibrations of the Neil Brown conductivity cell. *J. Phys. Oceanogr.*, **12**, 720–742.

Hansen, A. G., 1967: *Fluid Mechanics*. Wiley, 531 pp.

Horne, E. P. W., and J. M. Toole, 1980: Sensor response mismatches and lag correction techniques for temperature–salinity profilers. *J. Phys. Oceanogr.*, **10**, 1122–1130.

Huyer, A., P. M. Kosro, R. O'Malley, and J. Fleischbein, 1993: SEASOAR and CTD observations during COARE surveys cruise, W9211C, 22 January to 22 February 1993. Data Report 154, Ref. 93-2, 325 pp. [Available from the College of Oceanic and Atmospheric Sciences, Oregon State University, Corvallis, OR 97331-5503.]

Larson, N., 1989: The temperature and conductivity duct: Installation, use, and data processing steps to minimize salinity spiking error. Sea-Bird Electronics, Inc., 40 pp. [Available from 1808 136th Place N.E., Bellevue, WA 98005-2319.]

Lueck, R. G., 1990: Thermal inertia of conductivity cells: Theory. *J. Atmos. Oceanic Technol.*, **7**, 741–755.

——, and J. J. Picklo, 1990: Thermal inertia of conductivity cells: Observations with a Sea-Bird cell. *J. Atmos. Oceanic. Technol.*, **7**, 756–768.

Ochoa, J., 1989: A practical determination of CTD platinum resistance thermometer response time, and its use to correct salinity bias and spikes. *Deep-Sea Res.*, **36**, 139–148.